P-ISSN 2586-9000
E-ISSN 2586-9027
Homepage : https://tci-thaijo.org/index.php/SciTechAsia Science & Technology Asia
Vol.25 No.2 April - June 2020 Page: [47-62]
Original research article

Influence of the Jet Air Flow with Inclined Plate under Corona Discharge

Suwimon Saneewong Na Ayuttaya*

Department of Mechanical Engineering, Academic Division, Chulachomklao Royal Military Academy, Nakhon Nayok 26001, Thailand

Received 13 July 2019; Received in revised form 21 October 2019
Accepted 18 December 2019; Available online 29 June 2020

ABSTRACT

In this research paper, the influence of the jet air flow with an inclined plate is investigated under corona discharge. The number of electrodes is varied in the range 1 - 6. The high electrical voltage and angle of inclined plate are tested in a range of 0 – 30 kV and 0 – 90^{o}, respectively. The jet air flow is fixed at 1 m/s. The first part of the experimental results showed that the pressure, the gravity force and the impact velocity under corona discharge are increased with increasing electrical voltage, the number of electrodes and angle of the inclined plate. This is because the strength of corona discharge is increased by increasing the electrical voltage and number of the electrodes. The pressure ratio and gravity force ratio are decreased with an increasing angle of the inclined plate because the effect of trap of airflow is dominantly influenced by increasing the angle of inclined plate. In addition, the maximum pressure, the gravity force and the impact velocity under corona discharge are 2.11, 5.24 and 1.88 times, respectively, in comparison with no corona discharge. The second part of the comparison between experimental and numerical results showed that the pressure and the impact velocity under corona discharge are increased with an increasing electrical voltage and the angle of the inclined plate. The impact velocity under corona discharge is dominantly increased by the electrical voltage increasing. Finally, a similar trend of the graph has appeared for experimental and numerical results so simulation results had good agreement with experiment results.

Keywords: Jet air flow; Impact velocity; Corona discharge; Gravity force; Inclined plate

***Corresponding author:** joysuwimon@gmail.com **doi:** 10.14456/scitechasia.2020.20

1. Introduction

A coating is a covering that is applied to the surface of an object, usually referred to as the substrate. The coating itself may be an all-over coating, completely covering the substrate, or it may only cover parts of the substrate. Paints and lacquers are coatings that mostly have dual uses of protecting the substrate and being decorative, although some artists' paints are only for decoration, and the paint on large industrial pipes is presumably only for the function of preventing corrosion [1-3]. An aircraft painting coats [4-5] the exterior and interior of the airplane. Since appearances do matter, especially in aircraft, it is important to paint it with eye-catching colors and designs. The purpose of applying the coating may be decorative, functional, or both. The aircraft painting is coatings for the substrate, being decorative and preventing corrosion. The aircraft coating is a very detailed exercise due to the surface of an aircraft being subject to serious UV radiation; the surface itself being aluminum, which does not provide the mechanical key the paint needs to hold on to the surface; the temperatures the aircraft could face could be in extremes, and the paint applied should be able to take mechanical and thermal shock [6]. Therefore, the aircraft coating must use the science that is higher than normal coatings. Furthermore, spray painting is a painting technique where a device sprays a coating.

From mechanism characteristics, Saneewong Na Ayuttaya [7] divided the fourth group of Electrohydrodynamics (EHD) applications. The first group was to increase the flow mechanism; it was used for pumping and biomechanics application. The second group was the injection flow mechanism; it was used for droplet, electrospray, and microfluidics. The third group was inducing flow mechanism; it was used for electrostatic precipitator and actuator. The fourth group was mixing particle process; it was used for boiling and condensation, heat and mass transfer, heat exchanger and drying process. For the third group (inducing flow mechanism), the induced flow caused the total reaction to lean backward in the plane of rotation. This also reduced the perpendicular component of the total reaction and reduced total rotor thrust. The motion and precipitation of dust particles in electrostatic precipitation depended on the electric field, space charge, and gas flow field and dust particle properties. So, the electrostatic spray coating used inducing flow mechanism for aircraft painting. The electrostatic spray coating is a manufacturing process that employs charged particles to more efficiently paint a workpiece. Paint, in the form of either powdered particles or atomized liquid, is initially projected towards a conductive workpiece using normal spraying methods and is then accelerated toward the workpiece by a powerful electrostatic charge [8]. The ionic bond of the paint to the metal created the paint coating, whose thickness was directly proportional to the length of time the parts were left in the tank and the time the charge remained active. The method of electrostatically coating a substrate involved the substrate being brought to a coating station at which it was held substantially electrically isolated from its surroundings adjacent to a source of the particulate coating material. The substrate and the coating material were held at a potential difference to each other sufficient to coat the exposed surface of the substrate with particles of the coating material. Over the past decades, several researchers have tried to increase the performance of electrostatic spray coating [9-19]. Bierwagen and Tallman [9] investigated and focused on system flexibility, adhesion, solvent resistance, corrosion protection, and camouflage optics as determined over the coatings lifetime while taking into account the effects of UV exposure, hot and cold organic fluids, seawater, humidity and temperature cycling, mechanical stressing and abrasion. The differences between test performance and real use performance will be considered,

especially with respect to film application uniformity and film damage. Mayr and Barringer [14] compared and determined the improvement between the corona and triboelectric charging for electrostatic powder coating. Five sizes of sucrose were coated onto the crackers to determine the effect of particle size on coating efficiency. Three proteins, three carbohydrates, and one salt were analyzed to determine the effect of the composition. From the results, electrostatics improved transfer efficiency (TE) up to 27%, adhesion up to 40%, and reduced dust up to 99% over nonelectrostatic coating. As particle size increased, nonelectrostatic TE and adhesion increased, while dust decreased. The electrostatic TE increased and leveled off and adhesion and dust decreased with increasing particle size. Qingling et al. [18] studied dry powder technology to coat pellets with different coating materials ground into fine powders. Results of SEM indicated coating film could be better formed by increasing curing temperature or extending curing time. Dissolution tests showed that three different drug release profiles, including immediate release, sustained release and delayed release, were achieved by this coating technology with different coating formulations. The coating procedure could be shortened to within 120 min and the use of fluidized hot air was minimized, cutting down the overall cost dramatically compared to organic solvent coating and aqueous coating.

For several reasons, electrostatic spray coating has always improved the process performance for various industrial applications such as composite materials, biopharmaceutics and aircraft coatings. For military aircraft coating, the desired properties can be summarized as mechanical and chemical protection of the airframe with controlled electromagnetic emission and reflection properties. This research aims to studies the effect of angle of the inclined plate and electrical high voltage with jet air flow under corona discharge. The jet air flow (u_i) is fixed at 1 m/s. The parameters of the suitable design are the electrical voltage (V_0), angle of the inclined plate (θ) and the number of electrodes (n). All parameters for electrostatic spray coating are evaluated for the suitable design in the coatings industry in the future.

2. Governing Equation

The governing equations for the electrohydrodynamic force per unit volume f_E generated by the electric fields with strength E in airflow of dielectric permittivity ε, density ρ, and uniform temperature T can be expressed as [20]

$$\vec{f}_E = q\vec{E} - \frac{1}{2}\vec{E}^2\nabla\varepsilon + \frac{1}{2}\nabla\left[\vec{E}^2\left[\frac{\partial\varepsilon}{\partial\rho}\right]_T\rho\right], \quad (1)$$

where q is the space charge density in the fluid. From Eq.(1), three terms are the electrophoretic, dielectrophoretic and electrostrictive forces, respectively. In the first term, the electrophoretic force or Coulomb force results from the net uncharged within the fluid or ions injected from the electrodes. The electric field distribution is emitted from the electrode wire and induces to the ground. In the second term, the dielectrophoretic force is a consequence of inhomogeneity in the permittivity of the dielectric fluid due to the non-uniform electric field, temperature gradients, and phase differences. The last term, the electrostrictive force is caused by non-homogeneous electric field strength and the variation in dielectric constant with temperature and density [21].

The electric field distribution is computed by using Maxwell's equations (Eqs. (2), (3), (4) and (5)) listed below:

$$\nabla\cdot\varepsilon\vec{E} = q, \quad (2)$$

$$\vec{E} = -\nabla V, \quad (3)$$

$$\nabla\cdot J + \frac{\partial q}{\partial t} = 0, \quad (4)$$

$$J = qb\vec{E} + q\vec{u}, \quad (5)$$

where u is airflow velocity, V is electrical voltage, J is current density, b is ion mobility and t is time. The continuity and the Navier–Stokes equations which coupled with the Coulomb force equation are considered from Eqs. (6) and (7), respectively. They are expressed by:

$$\nabla \cdot \vec{u} = 0, \quad (6)$$

$$\rho\left[\frac{\partial \vec{u}}{\partial t} + (\vec{u} \cdot \nabla)\vec{u}\right] = -\nabla \vec{P} + \mu \nabla^2 \vec{u} + \vec{f}_E, \quad (7)$$

where P is pressure and μ is viscosity of air. The Reynolds number (Re) is an important dimensionless quantity in fluid mechanics used to predict flow patterns in different fluid flow situations, as shown in Eq.(8)

$$\mathrm{Re} = \frac{\rho \vec{u} d}{\mu} \quad (8)$$

where d is characteristic linear dimension.

2.1 Description of experimental setup

Schematic diagrams of the electrostatic spray coating for the two-dimensional and three-dimensional models for analysis are shown in Figs. 1 and 2, respectively. For experimental setup, the wind tunnel is mostly made of the acrylic plates. The dimensions of tunnel are 1.5 m (long) x 0.3 m (high) x 0.3 m (wide) and the outlet diameter of a nozzle jet is 1 cm. The jet air flow from the nozzle jet is supplied from a blower at 1 m/s (u_i = 1 m/s) and the air is moved in the cross-flow direction (the left to the right direction). The high voltage power supply (ACOPIAN model: NO30HP2M.-230) is used to create an electrical voltage and the electrical high voltage (V_0) is varied from 0 to 30 kV. The inclined plate is made of acrylic (the dimension of the inclined plate is fixed at 15x15 cm^2) and the angle of the inclined plate (θ) is varied in the range of 0 – 90°. The square copper electrode plate and the single rectangle ground plate are attached at the inclined plate. The dimensions of the square copper electrode plate and the rectangle ground plate are 0.5 × 0.5 cm^2 and 0.5 × 10 cm^2, respectively. The number of electrode plates (n) is varied in the range 1 – 6 and the gap between the square copper electrode plate and the single rectangle ground plate is fixed at 4 cm. In each test run, pressure (P_{EHD}), impact velocity (u_{EHD}) and gravity force ($F_{g,EHD}$) under corona discharge or EHD process is measured by a manometer, flow meter and load cell, respectively.

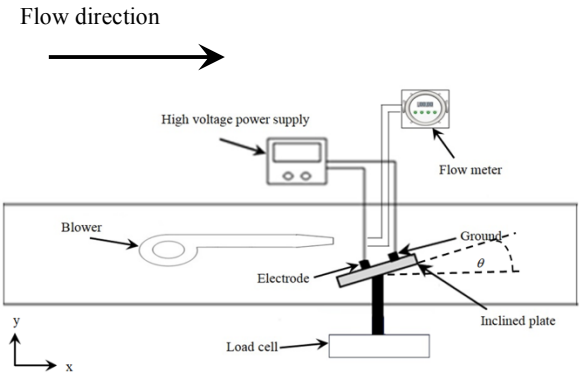

Fig. 1. Two-dimensional model for analysis.

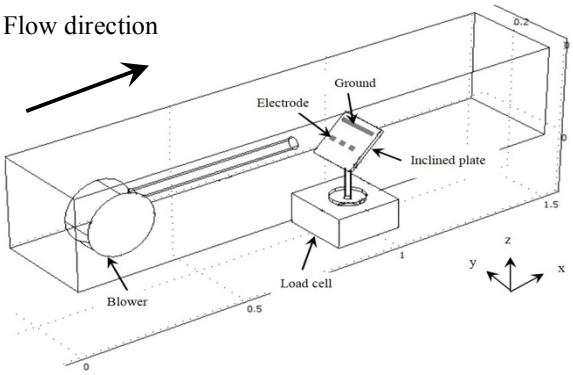

Fig. 2. Three-dimensional model for analysis.

The relative humidity is determined by the room's temperature, humidity, and airspeed. Radiant heat or radiant heat loss are also important factors for thermal comfort. The relative humidity is a measure of the moisture in the air, compared to the potential saturation level. Air temperature is a measure of the heat and most thermometers are measuring ambient air heat. The radiant heat loss or gain is also important. The radiant heat may not be reflected in the air temperature but is the impact of cold or hot objects in the area. In this study, the

saturation vapor pressure is 0.0028 – 0.0031 bar, the relative humidity is 58 – 62 % and the temperature of the condition experimental setup is controlled at 23 - 26 ^{o}C.

2.2 Description of numerical modeling

The numerical modeling has been formulated to predict the pressure and impact velocity within the rectangular duct. In fact, numerical modeling is a three-dimensional rectangular duct. In order to simply the description, two boundary conditions of the electric field and fluid flow are shown in Fig. 3. By using the electrical, charge transport and fluid equations are solved, the classical properties and the thermal properties are shown in Table 1 [22, 23].

Table 1. Classical and thermal properties.

Modeling parameter	Air	Water
$b(m^2/Vs)$	$1.80x10^{-4}$	-
$\varepsilon(F/m)$	$8.85x10^{-12}$	-
$\rho(kg/m^3)$	1.2	998
$\eta(m^2/s)$	$1.56x10^{-5}$	$1.005x10^{-5}$
k (W/mK)	0.026	0.588
C_p(kJ/kgK)	1.005	4.186

Where k is thermal conductivity, η is kinematics viscosity and C_p is specific heat capacity.

The modeling parameter of the airflow is a porous medium at 25 ^{o}C; it is a material containing voids and it is most often characterized by its porosity. The permeability of the medium can sometimes be derived from the respective properties of its constituents (air and fluid) and the pore space accessible to flow, but such a derivation is usually complex. So, the Brinkmann model is used for the effect of the porous medium. The computational scheme is assembled in a finite element model using a collocation method [24]. The Lagrange quadratic element is chosen as the basic function with triangular shapes. The convergence curve resulting from the convergence test is grid validation between percent error of electric field and different elements from the simulation. With a percentage error of temperature lower than 0.1, this convergence test leads to a mesh having approximately 15,000 elements.

For the model assumption of the electric field, this study is based on the dielectric property that is constant and homogeneous. In this numerical simulation, the first term of Eq. (1) is considered. In addition, the effect of the magnetic field is negligible and the corona discharge occurs only in the vicinity around the electrode. Boundary and initial condition of the electric field are based on the following:

(1) The outer sides of the boundary conditions are considered as zero charge symmetry, that is,

$$n \cdot D = 0. \quad (9)$$

(2) The electrical voltage at the tip of the electrode (V_0) is varied from 0 – 30 kV. The electrode and the ground are considered as electrical voltage and ground, respectively. Then

$$V = V_0, \text{ at electrode position}, \quad (10)$$

$$V = 0, \text{ at ground position}. \quad (11)$$

For the model assumption of the flow field, this study is based on the effect of the phase change being neglected, the incompressible flow and the fluid physical properties are assumed to be constant, and the effect of buoyancy and emission or absorption of radiant energy is negligible. The thermal properties of the air are considered to be constant and air is set in a porous medium.

The boundary condition of the flow field is based on the following:

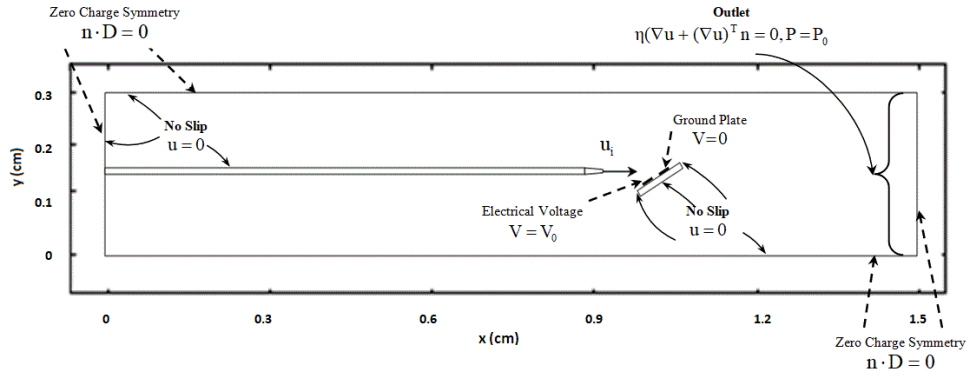

Fig. 3. Boundary conditions for analysis.

(1) The initial condition of jet air flow (u_i) = 1 m/s and the inlet velocity boundary condition of air is assumed to be uniform.

$$\vec{u} = \vec{u}_i . \qquad (12)$$

(1) The pressure of outlet boundary condition is considered with no viscous stress. This boundary condition specifies vanishing viscous stress along with a Dirichlet condition on the pressure:

$$\eta(\nabla\vec{u} + (\nabla\vec{u})^T \cdot n = 0 \text{ and } \vec{P} = \vec{P}_0 . \qquad (13)$$

(2) The upper and lower rectangular ducts are considered as a no-slip boundary condition; this is the standard and default boundary condition for a stationary solid wall. The condition prescribed:

$$\vec{u} = 0 . \qquad (14)$$

3. Results and Discussion

In this setup, the electrical voltage (V_0) is varied from 0 to 30 kV; it is incremented by 5 kV and the angle of the inclined plate (θ) is varied in the range of 0 – 90°; it is incremented by 15°. (for clarity, "o" from all the Figure is instead in "degree"). The number of electrode plates (n) is varied in the range 1 – 6. The experimental and numerical results are compared in order to investigate the pressure (P_{EHD}), the impact velocity (u_{EHD}) and the gravity force ($F_{g,EHD}$) under corona discharge.

Firstly, the experimental and numerical results with an inclined plate under corona discharge are investigated in order to confirm the accuracy of both results. After that, the experimental study of the pressure, the impact velocity and the gravity force under corona discharge are investigated and compared with no EHD or corona discharge in order to avoid considering the impact force of the inclined plate. A correlation is a statistical measure of the relationship between two variables [25]. The measure is best used in variables that demonstrate a linear relationship between each other. In this research study, the pressure under corona discharge (P_{EHD}), the electrical voltage (V_0), the impact velocity under corona discharge (u_i), the gravity force ratio under corona discharge ($F_{g,EHD}$ per $F_{g,noEHD}$), the impact velocity ratio under corona discharge (u_{EHD} per u_{noEHD}) and the Reynolds number under corona discharge (Re_{EHD}) are studied for correlation in order to guide the special design for the aircraft painting coats.

3.1 Comparison between the experimental and numerical result with inclined plate under corona discharge

The influence of the jet air flow with an inclined plate under corona discharge is investigated using both experimental and numerical results. The jet air flow (u_i) is fixed at 1 m/s and the air is moved from the left to the right direction. The electrical voltage (V_0) is tested from 0 to 30 kV by increments of 5. The number of electrode plates (n) is

fixed at 1 and the angle of the inclined plate (θ) is studied at 0, 45 and 90°. The pressure under corona discharge (P_{EHD}) and the impact velocity under corona discharge (u_{EHD}) are increased with increasing electrical voltage and the angle of inclined plate, as shown in Figs. 4 and 5, respectively. This is because as the electrical voltage of airflow is increased, the strength of corona discharge is increased. The pressure and impact velocity under corona discharge are dominantly increased when the angle of the inclined plate is 90° because increasing the angle of inclined plate increases the trap of airflow. A variable straight line for the pressure under corona discharge and electrical voltage ($P_{EHD} \propto V_0$) and the impact velocity under corona discharge is proportional to the square of the electrical voltage ($u_i \propto V_0^2$).

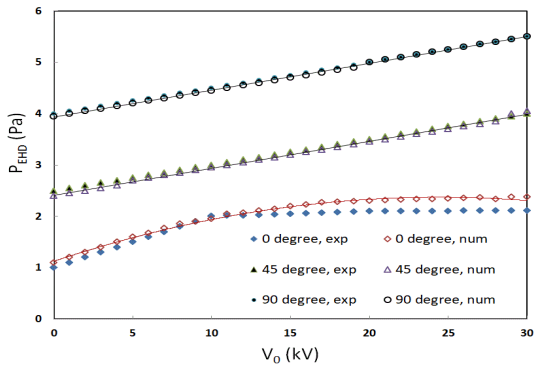

Fig. 4. Comparison of pressure between experimental and numerical result in various electrical voltage and angle of inclined plate (θ = 0°, 45°and 90°) when u_i = 1 m/s and n = 1.

From the previous study [26], the electric field is moving outward from the electrode to ground concentrating at both electrode and ground area. The maximum pressure and the maximum impact velocity have appeared between the electrode and ground area. The position for measuring is the middle of the inclined plate and between the electrode and ground area. The maximum impact velocity and the maximum pressure are clearly increased by increasing the electrical voltage and inlet velocity more than by increasing the number of electrodes (n). This experimental and numerical study has selected various electrical voltages and the number of the electrodes is fixed. So, in this comparison between the experimental and numerical result with an inclined plate under corona discharge, it is presented for n = 1. In addition, a similar trend of the graph has appeared for the experimental and numerical results so simulation results had good agreement with experiment results.

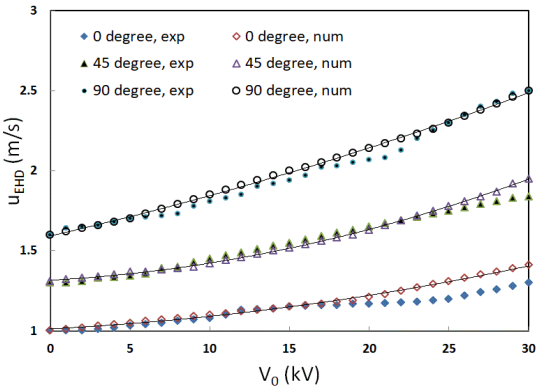

Fig. 5. Comparison of impact velocity between experimental and numerical result in various electrical voltage and angle of inclined plate (θ = 0°, 45°and 90°) when u_i = 1 m/s and n = 1.

3.2 Experimental study influence of the jet air flow with inclined plate under corona discharge

The airflow comes out in the form of a jet from the outlet of a nozzle, which is fitted to a pipe through which the air is flowing under pressure. If some plate, which may be fixed or moving, is placed in the path of the jet, a force is exerted by the jet on the plate. This force is obtained from Newton's second law of motion or from the impulse-moment equation. Thus, the impact of the jet means the force exerted by the jet on a plate which may be stationary or moving. During an impact, the energy of a moving object is converted into work and force plays an important role [27]. In this experimental study, pressure, impact velocity and gravity force under corona discharge are compared with no corona discharge in each angle of the

inclined plate. So pressure ratio (P_{EHD} per P_{noEHD}), impact velocity ratio (u_{EHD} per u_{noEHD}) and gravity force ratio (F_{gEHD} per $F_{g,noEHD}$) are experimentally investigated in the influence of the jet air flow with an inclined plate under corona discharge.

From the previous studies, Saneewong Na Ayuttaya and colleagues [28] were early investigators of the EHD process. EHD, also known as electro-fluid-dynamics or electrokinetics, is the study of the dynamics of electrically charged fluids. It is the study of the motions of ionized particles or molecules and their interactions with electric fields and the surrounding fluid. Its means, electric field and the flow field are the main compound of the EHD process so inlet velocity (jet air flow) is not neglected in this research paper. The jet air flow (u_i) is fixed at 1 m/s and air is moved from the left to the right direction. The electrical voltage (V_0) is tested from 0 to 30 kV and it increments by 5. The number of electrode plates (n) is varied from 1 to 6 and the angles of inclined plates (θ) are varied from 0 to 90^o and incremented by 15^o.

The pressure ratio under corona discharge per no corona discharge in each angle of inclined plate (P_{EHD} per P_{noEHD}) is compared in various electrical voltages and angles of the inclined plate, as shown in Fig.6. The number of electrodes (n) is fixed at 1. It can be seen that the pressure ratio is increased with increasing electrical voltage. This is because the strength of corona discharge is increased by increasing the electrical voltage. But the pressure ratio is decreased with an increasing angle of the inclined plate. The effect of trap of airflow is dominantly influenced by increasing the angle of the inclined plate. In addition, the pressure ratio is dominantly increased in case of $\theta = 0^o$. It is dominantly increased with the electrical voltage at 0 to 10 kV and it is gradually increased when electrical voltage more than 10 kV. In addition, the maximum pressure under corona discharge per no corona discharge in each angle of the inclined plate for $\theta = 0^o$, 15^o, 30^o, 45^o, 60^o, 75^o and 90^o are 2.11, 1.87, 1.75, 1.60, 1.50, 1.43 and 1.38 times, respectively.

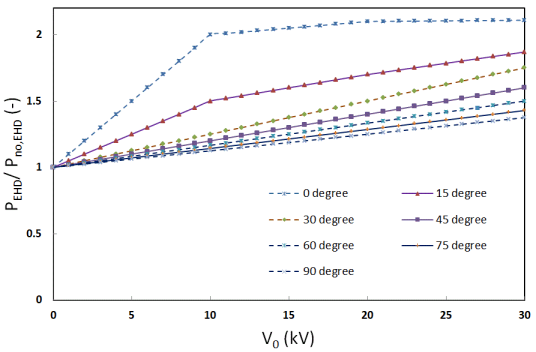

Fig. 6. Experimental comparison of pressure ratio in various electrical voltage and angle of inclined plate when u_i = 1 m/s and n = 1.

The gravity force ratio under corona discharge per no corona discharge in each angle of inclined plate ($F_{g,EHD}$ per $F_{g,noEHD}$) is compared for various electrical voltages and angles of inclined plate, as shown in Fig.7. The angle of inclined plate from $\theta = 0^o$, 15^o, 30^o, 45^o, 60^o, 75^o and 90^o is shown in Fig. 7 (a-g), respectively. It can be seen that the gravity force ratio is increased with increasing electrical voltage and the number of the electrodes. This is because the strength of corona discharge is increased by increasing the electrical voltage and number of electrodes but the gravity force ratio is decreased with an increasing angle of the inclined plate. Due to the effect of the trap of airflow is dominantly influenced by increasing the angle of inclined plate so gravity force in case of increasing the angle of inclined plate is more dominated than gravity force under corona discharge. The gravity force ratio under corona discharge from $\theta = 0^o$ (Fig. 7(a)) is increased more than $\theta = 90^o$ (Fig. 7 (g)). The maximum gravity force under corona discharge per no corona discharge in each angle of the inclined plate for $\theta = 0^o$, 15^o, 30^o, 45^o, 60^o, 75^o and 90^o are 5.24, 5.00, 4.76, 4.52, 4.30, 4.14 and 4.03 times, respectively. The

gravity force ratio under corona discharge is proportional to square of the electrical voltage ($F_{g,EHD}$ per $F_{g,noEHD} \propto V_0^2$).

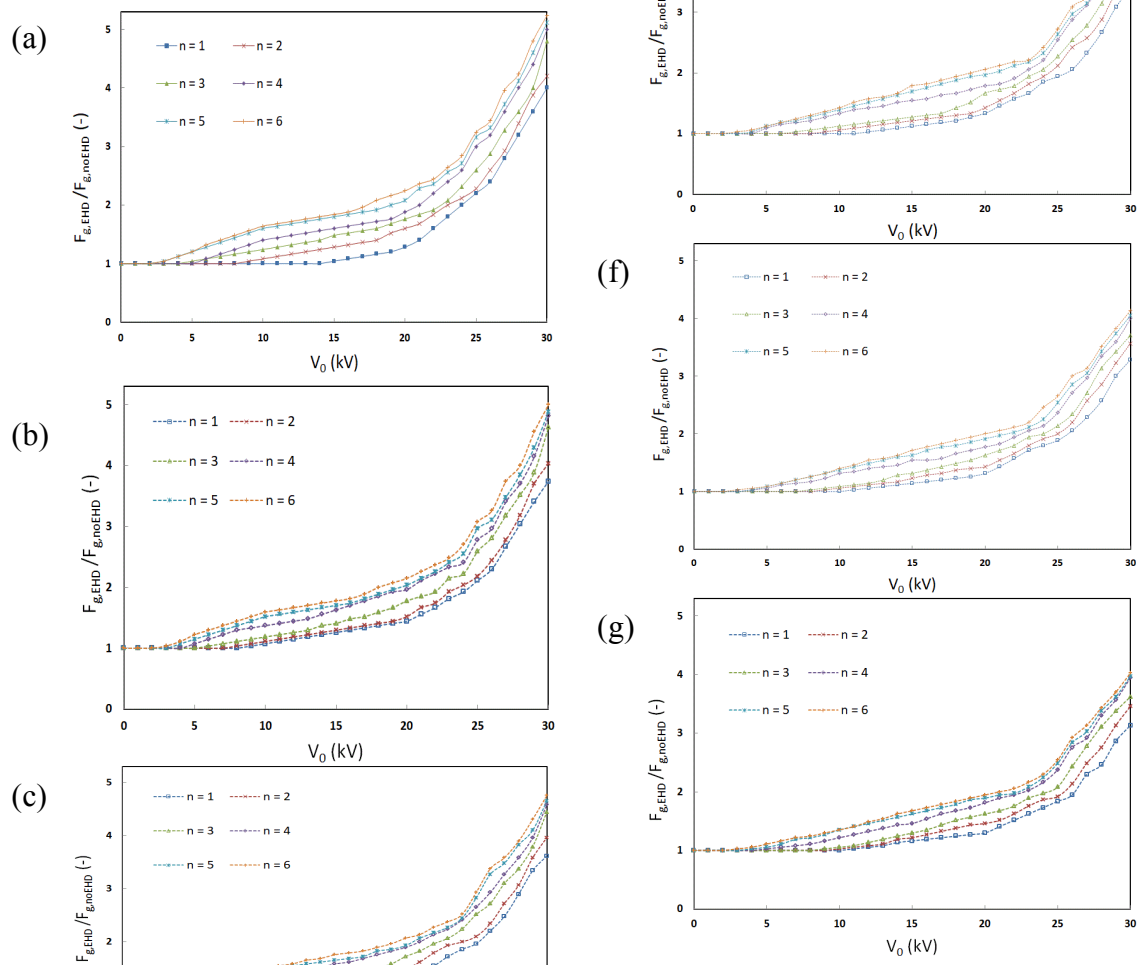

Fig. 7. Experimental comparison of gravity force ratio in various number of electrode and electrical voltage when u_i = 1 m/s (a) $\theta = 0^o$ (b) $\theta = 15^o$ (c) $\theta = 30^o$ (d) $\theta = 45^o$ (e) $\theta = 60^o$ (f) $\theta = 75^o$ and (g) $\theta = 90^o$.

The impact velocity ratio under corona discharge per no corona discharge in each angle of inclined plate (u_{EHD} per u_{noEHD}) is compared in various electrical voltages and angles of inclined plate, as shown in Fig.8. The angle of inclined plate from $\theta = 0^o$, 15^o, 30^o, 45^o, 60^o, 75^o and 90^o is shown in Fig. 8 (a-g), respectively. It can be seen that the impact velocity ratio is increased with

increasing electrical voltage and the number of electrodes. This is because the strength of corona discharge is increased by increasing the electrical voltage. The inertial force is supported by the electric force when the angle of the inclined plate is increased. The impact velocity ratio is gradually increased with increasing angle of inclined plate, the number of the electrode and electrical voltage. The maximum impact velocity under corona discharge per no corona discharge in each angle of inclined plate for $\theta = 0^o, 15^o, 30^o, 45^o, 60^o, 75^o$ and 90^o are 1.80, 1.82, 1.83, 1.84, 1.86, 1.87 and 1.88 times, respectively. A variable straight line is the impact velocity ratio under corona discharge and the electrical voltage (u_{EHD} per $u_{noEHD} \propto V_0$).

From the above results, the maximum pressure and the maximum gravity force under corona discharge per no corona discharge in each angle of the inclined plate are decreased with increasing the angle of inclined plate. This is because the EHD process or under corona discharge is not influenced by pressure increasing and the direction of gravity force is not the same direction with corona discharge direction. The corona discharge direction is supported with flow field direction and electric field direction; it is the x-axis direction but the gravity force is the y-axis direction. Inversely, the maximum impact velocity under corona discharge per no corona discharge in each angle of the inclined plate is increased with increasing the angle of the inclined plate. This is because the direction of impact velocity is supported with flow field direction and electric field direction from corona discharge.

(a)

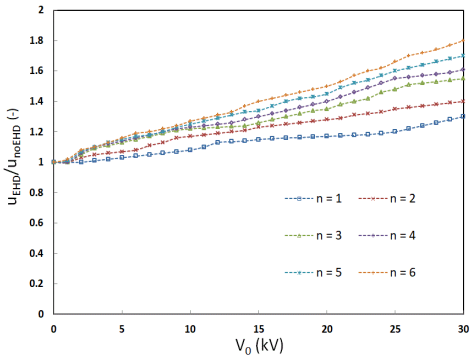

(b)

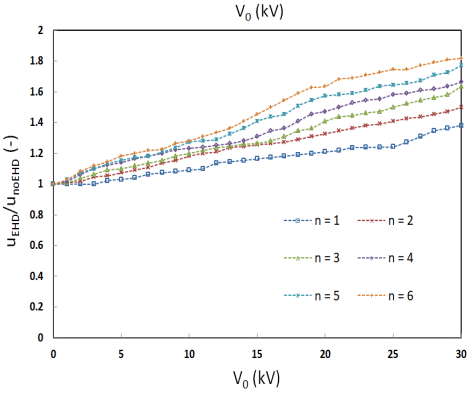

(c)

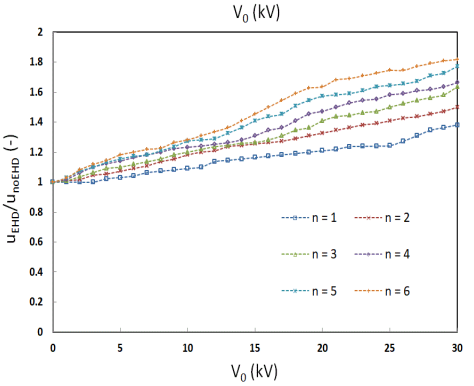

(d)

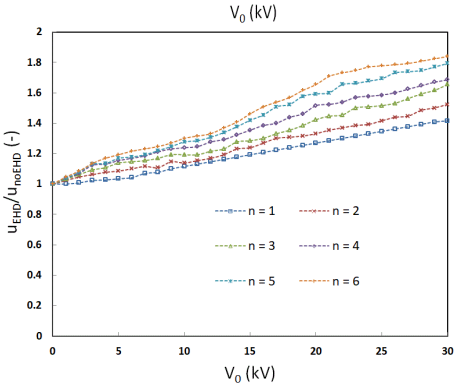

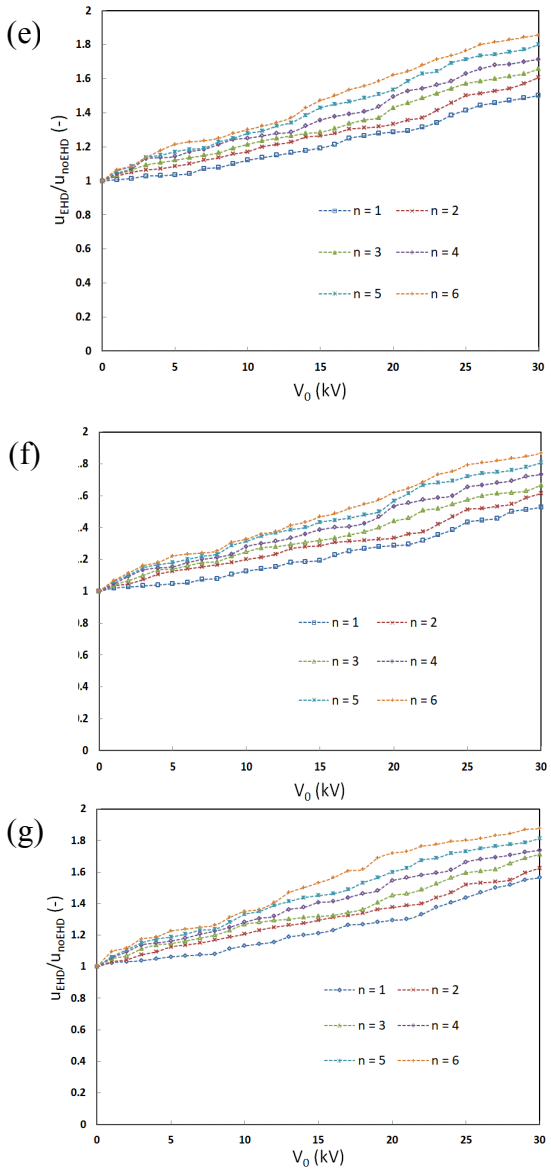

Fig. 8. Experimental comparison of impact velocity ratio in various number of electrode and electrical voltage when u_i = 1 m/s (a) $\theta = 0^o$ (b) $\theta = 15^o$ (c) $\theta = 30^o$ (d) $\theta = 45^o$ (e) $\theta = 60^o$ (f) $\theta = 75^o$ and (g) $\theta = 90^o$.

3.3 Discussion results of the jet air flow with inclined plate under corona discharge

From the above data, the pressure, the impact velocity and the gravity force under corona discharge per no corona discharge in each angle of the inclined plate are compared in various electrical voltages, the number of electrodes and angle of the inclined plate. In these paragraphs, the discussion results of the jet air flow with inclined plate under corona discharge are presented. The pressure (P_{EHD}), gravity force ($F_{g,EHD}$) and Reynolds number (Re_{EHD}) are experimentally investigated in the influence of the jet air flow with an inclined plate under corona discharge. The jet air flow (u_i) is fixed at 1 m/s and air is moved from the left to the right direction. The pressure under corona discharge (P_{EHD}) in each angle of inclined plate is compared in electrical voltage and angle of inclined plate when n = 1, as shown in Fig. 9. It can be seen that the pressure is increased with increasing electrical voltage and angle of the inclined plate. When the angle of the inclined plate is varied from 30 to 90°, the graph of pressure is a variable straight line for the electrical voltage under corona discharge.

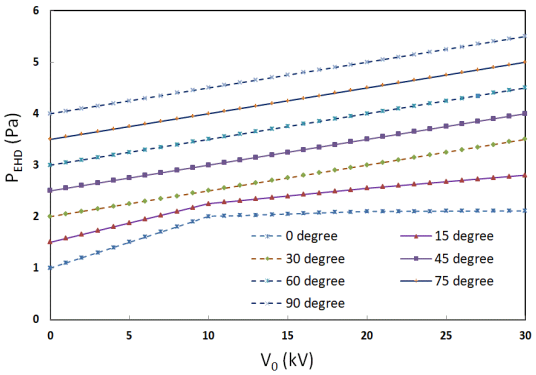

Fig. 9. Experimental comparison of pressure in various electrical voltage and angle of inclined plate when u_i = 1 m/s and n = 1.

The gravity force under corona discharge ($F_{g,EHD}$) is increased with increasing electrical voltage, angle of incline and number of electrodes, as shown in Fig. 10. The number of electrodes from n = 1, 3 and 5 is shown in Fig. 10 (a-c), respectively. It can be seen that gravity force is increased by increasing the number of electrodes. This is because the strength of corona discharge is increased by increasing the electrical voltage and number of electrodes. When $\theta = 0^o$, the gravity force under corona discharge is not

dominated due to it is not the trap of the airflow. The inertial force is supported by the electric force when the angle of the inclined plate is increased.

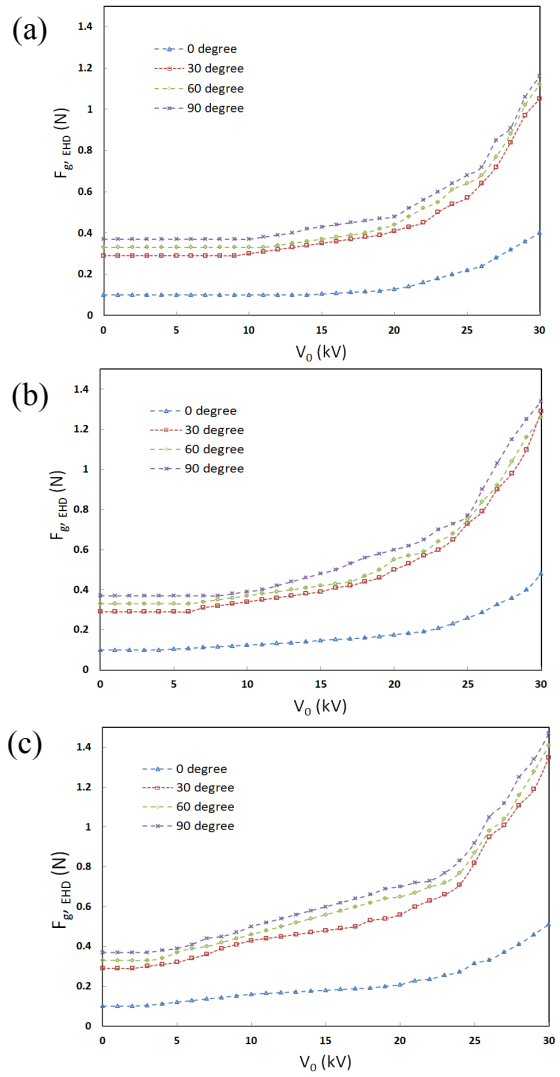

Fig. 10. Experimental comparison of gravity force in various electrical voltage and angle of inclined plate when u_i = 1 m/s (a) n = 1 (b) n = 3 and (c) n = 5.

The effect of trap of airflow is dominantly influenced by increasing the angle of the inclined plate. In addition, the gravity force under corona discharge ($F_{g,EHD}$) is increased with the number of electrode and angle of inclined, as shown in Fig. 11. It can be seen that gravity force under corona discharge is increased with increasing the number of electrodes and angle of the inclined plate but in the case of $\theta = 0^o$, the gravity force under corona discharge is not increased with increasing the number of the electrodes.

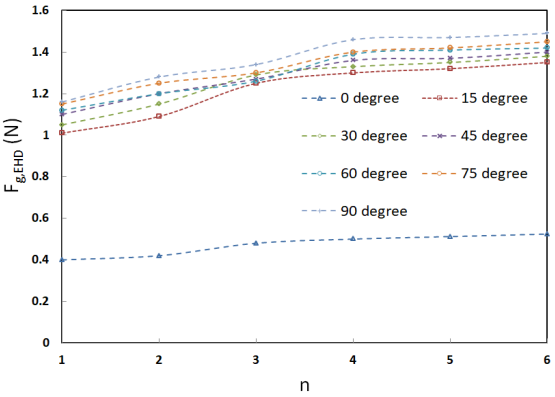

Fig. 11. Experimental comparison of gravity force in various number of electrode and angle of inclined plate when u_i = 1 m/s and V_0 = 30 kV.

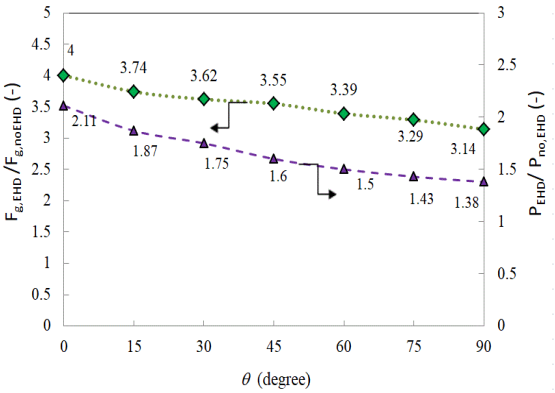

Fig. 12. Experimental comparison of gravity force ratio and pressure ratio in various angle of inclined plate when u_i = 1 m/s, n = 1 and V_0 = 30 kV.

The gravity force ratio ($F_{g,EHD}$ per $F_{g,noEHD}$) and pressure ratio (P_{EHD} per P_{noEHD}) under corona discharge per no corona discharge in each angle of inclined plate and is compared in various angles of the inclined plate, as shown in Fig. 12. The jet air flow (u_i) is fixed at 1 m/s, the number of electrode (n) equal 1 and the electrical voltage (V_0) is 30 kV. The pressure ratio and gravity force

ratio are decreased with an increasing angle of the inclined plate. This is because the effect of trap of airflow is dominantly influenced by increasing the angle of inclined plate.

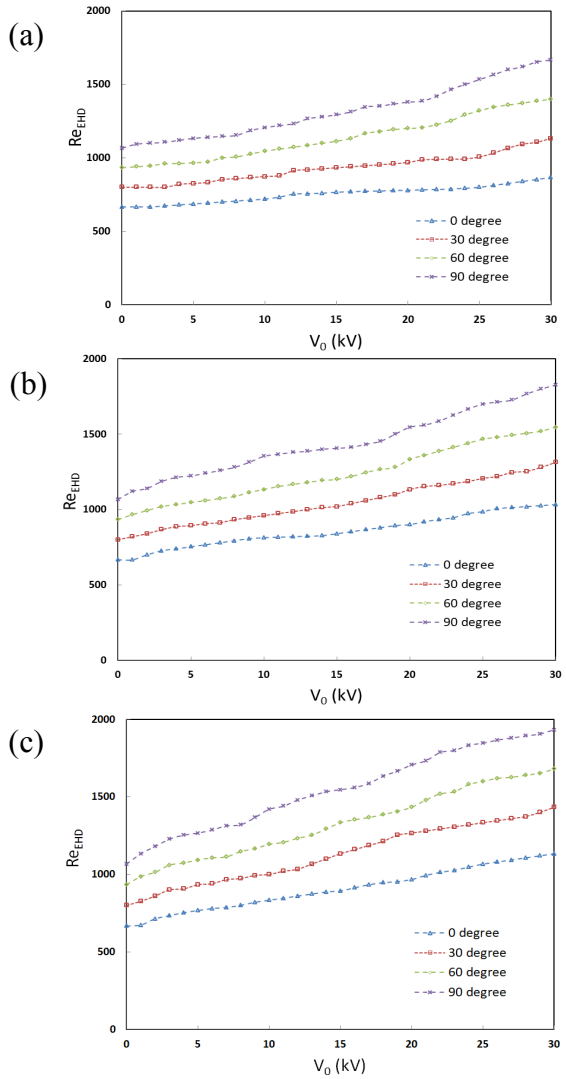

Fig. 13. Experimental comparison of Reynolds number in various electrical voltage and angle of inclined plate when u_i = 1 m/s (a) n = 1 (b) n = 3 and (c) n = 5.

Finally, the Reynolds number under corona discharge (Re_{EHD}) is increased with the number of the electrode, electrical voltage and angle of inclined plate, as shown in Figs. 13 and 14. Fig. 13 shows Reynolds number under corona discharge (Re_{EHD}) and electrical voltage with increasing the angle of the inclined plate. The angle of the inclined plate (θ) is varied from 0 to 90° in increments of 30°. It can be seen that Reynolds number under corona discharge is increased with increasing the electrical voltage and angle of the inclined plate. The number of electrodes from n = 1, 3 and 5 is shown in Fig. 13 (a-c), respectively. Reynolds number under corona discharge is increased with increasing the number of the electrode and the angle of the inclined plate.

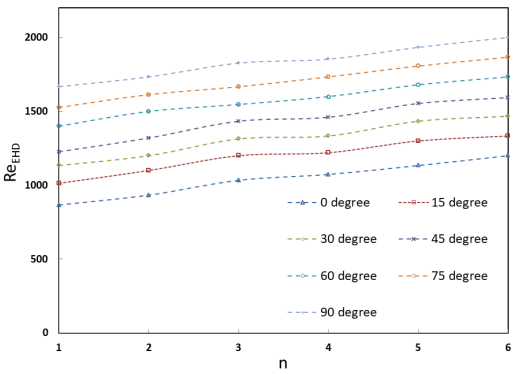

Fig. 14. Experimental comparison of Reynolds number in various number of electrode and angle of inclined plate when u_i = 1 m/s, n = 5 and V_0 = 30 kV.

Fig. 14 shows Reynolds number under corona discharge (Re_{EHD}) and the number of the electrode by increasing the angle of inclined plate. By the angle of inclined plate (θ) are varied from 0 to 90° and it increments by 15° and electrical voltage is fixed at 30 kV. The Reynolds number under corona discharge per no corona discharge in each the angle of the inclined plate for θ = 0°, 15°, 30°, 45°, 60°, 75° and 90° are 1200, 1333, 1466, 1593, 1733, 1866 and 2000, respectively when n = 6. In all cases, Reynolds number under corona discharge is increased with increasing the angle of the inclined plate it can be seen that Laminar flow generally occurs when the fluid is moving slowly or the fluid is very viscous. A variable straight line is the Reynolds number under corona

discharge and electrical voltage ($Re_{EHD} \propto V_0$).

In order to guarantee the parameter for aircraft painting design, the parameters are shown by using the correlation. From the above results, it can be seen that the pressure under corona discharge and the electrical voltage is $P_{EHD} \propto V_0$, the impact velocity under corona discharge and the square of electrical voltage is $u_i \propto V_0^2$, the gravity force ratio under corona discharge and the electrical voltage is $F_{g,EHD}$ per $F_{g,noEHD} \propto V_0^2$, the impact velocity ratio under corona discharge and the electrical voltage is u_{EHD} per $u_{noEHD} \propto V_0$ and the Reynolds number under corona discharge and electrical voltage is $Re_{EHD} \propto V_0$ in order to guide for special design for the aircraft painting coats.

4. Conclusion

The numerical and experimental result is carried out to study the influence of the jet air flow with an inclined plate investigated under corona discharge. The following are the conclusions of this work:

1. The pressure, the gravity force and the impact velocity under corona discharge are increased with increasing electrical voltage, the number of electrodes and the angle of inclined plate.

2. When the comparison between the corona discharge condition and no corona discharge condition in each angle of the inclined plate is made, the pressure ratio is increased with increasing electrical voltage, the gravity force ratio and impact velocity ratio are increased with increasing electrical voltage and number of electrodes. In addition, the pressure ratio and gravity force ratio are decreased but the impact velocity ratio is increased with increasing angle of the inclined plate.

From the above data, the idea behind this work can be used as guidance for special design for the aircraft painting coats. The corona discharge or Electrohydrodynamics process is designed for military aircraft with the least manpower and minimum maintenance in the future.

Acknowledgements

The authors gratefully acknowledge the Chulachomklao Royal Military Academy Fund and Department of Mechanical Engineering, Faculty of Engineering, Rajamangala University of Technology Rattanakosin for their support of this study.

Nomenclatures

b	ion mobility (m^2/Vs)
C_p	specific heat capacity (J/kgK)
D	electric flux density (C/m^2)
d	characteristic linear dimension (m)
E	electric field intensity (V/m)
EHD	Electrohydrodynamics
f_E	electric force (C/m^2s)
F_g	gravity force (N)
J	current density (A/m^2)
k	thermal conductivity (W/mK)
n	number of electrode plate, unit vector
P	pressure (N/m^2)
q	space charge density (C/m^3)
Re	Reynolds number (-)
T	uniform temperature (K)
t	time (hr)
u	airflow velocity (m/s)
V	electrical voltage (V)
x, y, z	axis

Greek letters

ε	dielectric permittivity (F/m)
θ	angle of the inclined plate $(^\circ)$
μ	viscosity (kg/ms)
η	kinematics viscosity (m^2/s)
ρ	density (kg/m^3)

Subscripts

i	inlet
0	initial

Superscripts

T transpose matrix

References

[1] Chamaimon B, Satok C. Thermal Energy Analysis for Sulfuric Acid Dilution Step in Copper Electroplating Process. Thammasat Int J of Sci and Tech 2010;15:55-59.

[2] Gordon B, Roger B, Dante B, Scott H. Active Metal-Based Corrosion Protective Coating Systems for Aircraft Requiring No-Chromate Pretreatment, Prog Org Coat 2010;67(2):195-20.

[3] Rigney DV, Viguie R, Wortman DJ, Skelly DW. PVD Thermal Barrier Coating Applications and Process Development for Aircraft Engines. J Therm Spray Techol 1997;6(2):167-175.

[4] Kiran VM. Colourant Performance and Fastness Assessment of 1, 3-diaryl 1, 2-propen-1-one Compounds on Synthetic Fabrics. Thammasat Int J of Sci and Tech 2012;17(3):34-39.

[5] Shi-Nian U, Tung-Sheng S, Chun-Huei C, Szu-Min C, Chuen-Jinn T, Deshpande CG. Exposure Assessment of Organic Solvents for Aircraft Paint Stripping and Spraying Workers. Sci Total Environ 2006;356(1-3):38-44.

[6] Peter TL, Bolch WE. The Impact of Recirculating Industrial Air on Aircraft Painting Operations. J Appl Occ and Envi Hyg 1999;14(10):682-690.

[7] Saneewong Na Ayuttaya S. A Review of Electrohydrodynamics Application (Based on the Mechanism Characteristic). J of CRMA 2017;15:37-59.

[8] Ye Q, Steigleder T, Scheibe, A, Domnick, J. Numerical Simulation of the Electrostatic Powder Coating Process with a Corona Spray Gun. J Electrost 2002;54:189-205.

[9] Bierwagen GP, Tallman DE. Choice and Measurement of Crucial Aircraft Coatings System Properties, Pro Org Coatings 2002;41(4):201-216.

[10] Ye Q, Domnick J. On the Simulation of Space Charge in Electrostatic Powder Coating with a Corona Spray Gun. Powder Technol 2002;135-136:250-260.

[11] Schmitt C., Lebienvenu, M. Electrostatic Painting of Conductive Composite Materials, J Mat Pro Technol 2003;134(3):303-309.

[12] Mark A, Andersson B, Tafuri S, Engstrom K, Sorod H, Edelvik F, Carlson JS. Simulation of Electrostatic Rotary Bell Spray Painting in Automotive Paint Shops, Atomiz Spr 2003;23(1):25-45.

[13] Joachim D, Andreas S, Qiaoyan Y. The Simulation of the Electrostatic Spray Painting Process with High-Speed Rotary Bell Atomizers. Part I: Direct Charging, Part Part Syst Charact 2005;22(2):141-150.

[14] Mayr MB, Barringer SA. Corona Compared with Triboelectric Charging for Electrostatic Powder Coating, J Food Sci 2006;71(4):171-177.

[15] Halim F., Barringer SA. Electrostatic adhesion in food, J Electrost 2007;65(3):168-173.

[16] Massimiliano B, Annamaria G. Electrostatic Spray Painting of Carbon Fibre-Reinforced Epoxy Composites, Pro Org Coatings 2009;64(4):339-349.

[17] Husam O, Peter Castle GS, Kazimierz A. Numerical Study of Particle Deposition in Electrostatic Painting near a Protrusion or Indentation on a Planar Surface, J Electrost 2015;77:58-68.

[18] Qingling Y, Yingling M, Jesse Z. Applying a Novel Electrostatic Dry Powder Coating Technology to Pellets, Eur J Pharm Biopharm 2015;97(A):118-124.

[19] Rui D, Yan S, Shuanglin L, Bo Y, Mangbo Y. Structuring Tri-Continuous Structure Multiphase Composites with Ultralow Conductive Percolation Threshold and Excellent Electromagnetic Shielding Effectiveness using Simple Melt Mixing, Int J Sci Technol Polymer 2016;83:34-39.

[20] David JG. Introduction to Electrohydrodynamics. Prentice Hall International,Inc. New Jersey; 1999. p. 105.

[21] Landau LD, Lifshitz EM. Electrohydrodynamics of Continuous Media. Pergamon, New York; 1963.

[22] Saneewong Na Ayuttaya S, Chaktranond C, Rattanadecho P, Kreewatcharin T. Effect of Ground Arrangements on Swirling Flow in a Channel Subjected to Electrohydrodynamic Effects, ASME J Fluids Eng 2012;134:051211-9.

[23] Sungsoontorn S, Rattanadecho P, Pakdee W. One-Dimensional Model of Heat and Mass Transports and Pressure Built Up in Unsaturated Porous Materials Subjected to Microwave Energy, Drying Technol 2011;29:189-204.

[24] COMSOL Inc., COMSOL Multi Physics Modeling Guide.

[25] Nikhil B. Avrim B, Shuchi C. Correlation Clustering, J Mach Lear Res 2004;56(1-3):89-113.

[26] Saneewong Na Ayuttaya S, Chaktranond C, Rattanadecho, P. Numerical Analysis of Electric force Influence on Heat Transfer in a Channel Flow (Theory Based on Saturated Porous Medium Approach), Int J Heat Mass Transfer;2013:64:361-374.

[27] Shinzo O, Yoichi, Sumi. On the Water Impact and Elastic Response of a Flat Plate at Small Impact Angles, J Mar Sci Technol 2000;5(1):31-39.

[28] Saneewong Na Ayuttaya S, Chaktranond C, Rattanadecho P. Flow Control with Electrode Bank Arrangements Electrohydrodynamics Force for Heat Transfer Enhancement in a Porous Medium, Heat Trans Asian Res 2018;47 (4): 620-645.